Paper

Ternary Cellular Automata with Three Neighbors

YOSHINORI NAGAI[a], ADRIAN ANKIEWICZ[b], and TED MADDESS[c]

(Received 25 Dec 2002, Revised 24 Jan 2003)

Synopsis: The class of cellular automata describing by three symbols is named Ternary Cellular Automata. A general rule description for these Ternary Cellular Automata is presented. Since Ternary Cellular Automata include Binary Cellular Automata, the Ternary Cellular Automata can be explained by a scheme of interactions between different kinds of Binary Cellular Automata. Some interesting spatio-temporal patterns in Ternary Cellular Automata are shown.

1. Introduction

Ternary cellular automata discussed here are cellular automata with three level states. A group of neighboring cells determines the next time state level of the centrally sited cell. In the present paper, we restrict our consideration to 3 neighbor cases. Thus here we treat the 3-neighbors 3-level cellular automata (CA_3^3) only. A few examples of CA_3^3 had been investigated, namely, patterns based on some totalistic rules (Wolfram [1]) and some other patterns based on totalistic rules are seen in a book [2]. We investigate CA_3^3 more systematically. In particular, we have studied the rule description for cellular automata in a general sense using a matrix form in [3] and recurrence formulae in [4]. We show the CA_3^3 rules in section 2.

The temporal development of cell states for CA_3^3 is described by the following recurrence equation,

$$S_i(t+1)=f(S_{i-1}(t),\ S_i(t),\ S_{i+1}(t)), \tag{1}$$

where $S_i(t)$ signifies the i-th cell state at time t. We describe a mapping f: $(S_{i-1}(t), S_i(t), S_{i+1}(t)) \rightarrow S_i(t+1)$ as a "rule". The total number of CA_3^3 rules is 3^W where $W=3^3$, i.e., 3^{27}. Hence a complete numerical study of temporal patterns for all CA_3^3 rules would be difficult. Wolfram had performed a complete study of the temporal patterns for all the rules of 3-neighbor 2-level cellular automata (CA^2_3) [5], since the number of rules is so much smaller. The temporal development of cell states in a cell array, i.e., temporal pattern, is called the "spatio-temporal pattern". Thus we analyzed CA_3^3 rules to study the CA_3^3 spatio-temporal patterns. We then revealed that the rule structure of CA_3^3 can be illustrated schematically as in Figure 1. The $\{-1, 1\}$, $\{-1, 0\}$, and $\{0, 1\}$ in Fig. 1 mean binary input triplets such as e.g. $(-1\ 1\ -1)$ for $\{-1, 1\}$, $(0\ -1\ -1)$ for $\{-1, 0\}$, $(1\ 1\ 0)$ for $\{0, 1\}$. All the input triplets are

[a]Center for Information Science, and Faculty of Political Science & Economy, Kokushikan University, [b]Applied Photonics Group, RSPhysSE, Australian National University, and [c]Centre for Visual Sciences, Research School of Biology, Australian National University

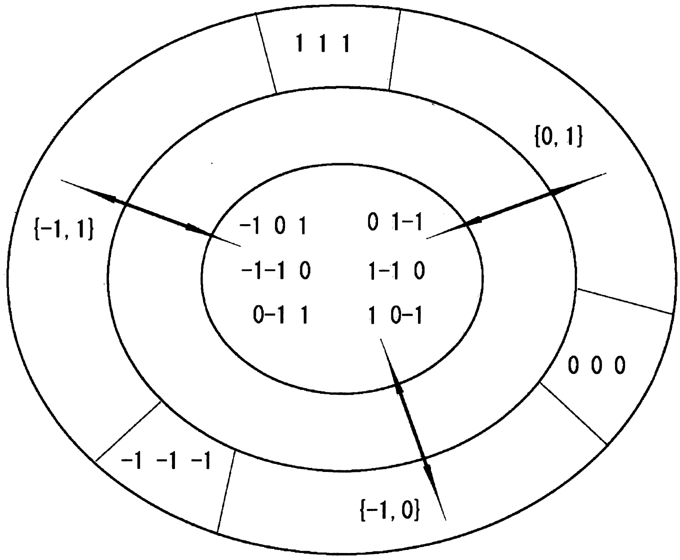

Figure 1 Schematic Description of CA_3^3 Rule Structure

tabulated in Table 1. The special input triplets $(-1\ -1\ -1)$, $(0\ 0\ 0)$, and $(1\ 1\ 1)$ are bridges between two CA_3^2 systems. The central zone in Fig. 1 denotes ternary input triplet of mapping, i.e., $(S_{i-1}(t), S_i(t), S_{i+1}(t))$. As expected, the CA_3^3 includes CA_3^2 of binaries $\{-1, 1\}$, $\{-1, 0\}$, and $\{0, 1\}$. This inclusion relation can be extended to the general case, that is $CA_{m'}^{L'} \subseteq CA_m^L$ where $L \geq L'$ and $m \geq m'$.

As expected from the scheme shown in Fig. 1, we found local-binary CA patterns where complicated patterns of CA_3^2 are separated by gray stripes (Figure 2). In principle, there should be globally ternary patterns, i.e. triple state levels coexisting everywhere in spatio-temporal patterns. We also found a moving soliton in CA_3^3, namely, the unit $(1\ -1)$, which moves to the right in the array $(0\ldots0\ 1\ -1\ 0\ldots0)$, and the unit $(-1\ 1)$, which moves to the left in the array $(0\ldots0\ -1\ 1\ 0\ldots0)$ [4]. Examples of spatio-temporal ternary CA patterns of Wolfram type are shown in section 3. We briefly summarize the present study for Ternary Cellular Automata in section 4.

2. Rule Description for Ternary Cellular Automata of Neighborhood Three

As stated above, the rule for CA_3^3 indicates the mapping of an input triplet state to the output state of the center cell, as shown in eq. (1). For the ternary case, the number of input triplet states is $3^3 = 27$. The output state takes one of three levels, so that the number of possible mappings from input triplet states $(S_{i-1}(t), S_i(t), S_{i+1}(t))$ to output cell state $S_i(t+1)$ amounts to $3^{27} \cong 7.6256 \times 10^{12}$. The output cell states are symbolically denoted by r_k for k-th state of the input triplet. We assume that state levels are assigned to the three integers $\{-1,$

0, 1}. Each r_k therefore takes one of these three integer values, so that $r_k \in \{-1, 0, 1\}$. These are tabulated (Table 1). The output states for essentially ternary input are assigned to r_6, r_8, r_{12}, r_{16}, r_{20}, and r_{22}. The outgoing arrows from triplets of the central zone in Figure 1 imply outputs r_6, r_8, r_{12}, r_{16}, r_{20}, and r_{22}. The bridging input triplets between any two of three $CA_3{}^2$ systems are r_1, r_{14}, and r_{27}. The output components of rules in three $CA_3{}^2$ are

$$\{r_1, r_3, r_7, r_9, r_{19}, r_{21}, r_{25}, r_{27}\} \quad \text{for } \{-1, 1\} \text{ in } CA_3{}^2 \text{ class,} \tag{2}$$
$$\{r_1, r_2, r_4, r_5, r_{10}, r_{11}, r_{13}, r_{14}\} \quad \text{for } \{-1, 0\} \text{ in } CA_3{}^2 \text{ class,} \tag{3}$$
$$\{r_{14}, r_{15}, r_{17}, r_{18}, r_{23}, r_{24}, r_{26}, r_{27}\} \quad \text{for } \{0, 1\} \text{ in } CA_3{}^2 \text{ class.} \tag{4}$$

Table 1 gives the complete classification of output components of $CA_3{}^3$.

Following our previous studies [3,4], the rule for $CA_3{}^3$, that is the mapping of input triplet states to an output state level, is expressed as follows:

$$\begin{aligned}
f(S_{i-1}(t), S_i(t), S_{i+1}(t)) = {} & x_{000} + x_{100}S_{i-1}(t) + x_{010}S_i(t) + x_{001}S_{i+1}(t) \\
& + x_{110}S_{i-1}(t)S_i(t) + x_{101}S_{i-1}(t)S_{i+1}(t) + x_{011}S_i(t)S_{i+1}(t) \\
& + x_{200}S_{i-1}^2(t) + x_{020}S_i{}^2(t) + x_{002}S_{i+1}^2(t) \\
& + x_{210}S_{i-1}^2(t)S_i(t) + x_{201}S_{i-1}^2(t)S_{i+1}(t) + x_{021}S_i{}^2(t)S_{i+1}(t) \\
& + x_{120}S_{i-1}(t)S_i{}^2(t) + x_{102}S_{i-1}(t)S_{i+1}^2(t) + x_{012}S_i(t)S_{i+1}^2(t) + x_{111}S_{i-1}(t)S_i(t)S_{i+1}(t) \\
& + x_{220}S_{i-1}^2(t)S_i{}^2(t) + x_{202}S_{i-1}^2(t)S_{i+1}^2(t) + x_{022}S_i{}^2(t)S_{i+1}^2(t) \\
& + x_{211}S_{i-1}^2(t)S_i(t)S_{i+1}(t) + x_{121}S_{i-1}(t)S_i{}^2(t)S_{i+1}(t) + x_{112}S_{i-1}(t)S_i(t)S_{i+1}^2(t) \\
& + x_{221}S_{i-1}^2(t)S_i{}^2(t)S_{i+1}(t) + x_{212}S_{i-1}^2(t)S_i(t)S_{i+1}^2(t) + x_{122}S_{i-1}(t)S_i{}^2(t)S_{i+1}^2(t) \\
& + x_{222}S_{i-1}^2(t)S_i{}^2(t)S_{i+1}^2(t)
\end{aligned} \tag{6}$$

$$= \Sigma_\alpha \Sigma_\beta \Sigma_\gamma x_{\alpha\beta\gamma} S_{i-1}^\alpha(t) S^\beta{}_i(t) S_{i+1}^\gamma(t) \tag{7}$$

$$\begin{aligned}
= {} & r_1(S_{i-1}^2(t) - S_{i-1}(t))(S_i{}^2(t) - S_i(t))(S_{i+1}^2(t) - S_{i+1}(t))/8 \\
& + r_2(S_{i-1}^2(t) - S_{i-1}(t))(S_i{}^2(t) - S_i(t))(1 - S_{i+1}^2(t))/4
\end{aligned}$$

Table 1 Rule Components Assignment to Input Triplets

Input Triplets			Output	Input Triplets			Output	Input Triplets			Output
Time t			t+1	Time t			t+1	Time t			t+1
S_{i-1}	S_i	S_{i+1}	S_i	S_{i-1}	S_i	S_{i+1}	S_i	S_{i-1}	S_i	S_{i+1}	S_i
−1	−1	−1	r_1	0	−1	−1	r_{10}	1	−1	−1	r_{19}
−1	−1	0	r_2	0	−1	0	r_{11}	1	−1	0	r_{20}
−1	−1	1	r_3	0	−1	1	r_{12}	1	−1	1	r_{21}
−1	0	−1	r_4	0	0	−1	r_{13}	1	0	−1	r_{22}
−1	0	0	r_5	0	0	0	r_{14}	1	0	0	r_{23}
−1	0	1	r_6	0	0	1	r_{15}	1	0	1	r_{24}
−1	1	−1	r_7	0	1	−1	r_{16}	1	1	−1	r_{25}
−1	1	0	r_8	0	1	0	r_{17}	1	1	0	r_{26}
−1	1	1	r_9	0	1	1	r_{18}	1	1	1	r_{27}

$$
\begin{aligned}
&+r_3(S_{i-1}^2(t)-S_{i-1}(t))(S_i^2(t)-S_i(t))(S_{i+1}^2(t)+S_{i+1}(t))/8\\
&\qquad +r_4(S_{i-1}^2(t)-S_{i-1}(t))(1-S_i^2(t))(S_{i+1}^2(t)-S_{i+1}(t))/4\\
&+r_5(S_{i-1}^2(t)-S_{i-1}(t))(1-S_i^2(t))(1-S_{i+1}^2(t))/2\\
&\qquad +r_6(S_{i-1}^2(t)-S_{i-1}(t))(1-S_i^2(t))(S_{i+1}^2(t)+S_{i+1}(t))/4\\
&+r_7(S_{i-1}^2(t)-S_{i-1}(t))(S_i^2(t)+S_i(t))(S_{i+1}^2(t)-S_{i+1}(t))/8\\
&\qquad +r_8(S_{i-1}^2(t)-S_{i-1}(t))(S_i^2(t)+S_i(t))(1-S_{i+1}^2(t))/4\\
&+r_9(S_{i-1}^2(t)-S_{i-1}(t))(S_i^2(t)+S_i(t))(S_{i+1}^2(t)+S_{i+1}(t))/8\\
&\qquad +r_{10}(1-S_{i-1}^2(t))(S_i^2(t)-S_i(t))(S_{i+1}^2(t)-S_{i+1}(t))/4\\
&+r_{11}(1-S_{i-1}^2(t))(S_i^2(t)-S_i(t))(1-S_{i+1}^2(t))/2\\
&\qquad +r_{12}(1-S_{i-1}^2(t))(S_i^2(t)-S_i(t))(S_{i+1}^2(t)+S_{i+1}(t))/4\\
&+r_{13}(1-S_{i-1}^2(t))(1-S_i^2(t))(S_{i+1}^2(t)-S_{i+1}(t))/2\\
&\qquad +r_{14}(1-S_{i-1}^2(t))(1-S_i^2(t))(1-S_{i+1}^2(t))\\
&+r_{15}(1-S_{i-1}^2(t))(1-S_i^2(t))(S_{i+1}^2(t)+S_{i+1}(t))/2\\
&\qquad +r_{16}(1-S_{i-1}^2(t))(S_i^2(t)+S_i(t))(S_{i+1}^2(t)-S_{i+1}(t))/4\\
&+r_{17}(1-S_{i-1}^2(t))(S_i^2(t)+S_i(t))(1-S_{i+1}^2(t))/2\\
&\qquad +r_{18}(1-S_{i-1}^2(t))(S_i^2(t)+S_i(t))(S_{i+1}^2(t)+S_{i+1}(t))/4\\
&+r_{19}(S_{i-1}^2(t)+S_{i-1}(t))(S_i^2(t)-S_i(t))(S_{i+1}^2(t)-S_{i+1}(t))/8\\
&\qquad +r_{20}(S_{i-1}^2(t)+S_{i-1}(t))(S_i^2(t)-S_i(t))(1-S_{i+1}^2(t))/4\\
&+r_{21}(S_{i-1}^2(t)+S_{i-1}(t))(S_i^2(t)-S_i(t))(S_{i+1}^2(t)+S_{i+1}(t))/8\\
&\qquad +r_{22}(S_{i-1}^2(t)+S_{i-1}(t))(1-S_i^2(t))(S_{i+1}^2(t)-S_{i+1}(t))/4\\
&+r_{23}(S_{i-1}^2(t)+S_{i-1}(t))(1-S_i^2(t))(1-S_{i+1}^2(t))/2\\
&\qquad +r_{24}(S_{i-1}^2(t)+S_{i-1}(t))(1-S_i^2(t))(S_{i+1}^2(t)+S_{i+1}(t))/4\\
&+r_{25}(S_{i-1}^2(t)+S_{i-1}(t))(S_i^2(t)+S_i(t))(S_{i+1}^2(t)-S_{i+1}(t))/8\\
&\qquad +r_{26}(S_{i-1}^2(t)+S_{i-1}(t))(S_i^2(t)+S_i(t))(1-S_{i+1}^2(t))/4\\
&+r_{27}(S_{i-1}^2(t)+S_{i-1}(t))(S_i^2(t)+S_i(t))(S_{i+1}^2(t)+S_{i+1}(t))/8. \qquad (8)
\end{aligned}
$$

Note that $S_i^2(t)$ means the product $S_i(t)\times S_i(t)$. Each term of eq. (8) behaves in a point-wise way. In other words, the function factor in each term, which is multiplied by rule component r_k, $k\in\{1, 2, 3, \ldots, 27\}$, takes value 1 only for the proper particular input triplet specified by the function factor.

Equivalency of formulae (6) and (8) leads to the fact that the $x_{\alpha\beta\gamma}$ coefficients are determined by the rule $(r_1, r_2, r_3, \ldots, r_{27})$. The description of the $x_{\alpha\beta\gamma}$ coefficients in terms of the rule components $r_1, r_2, r_3, \ldots, r_{27}$ are obtained by this equivalency (see [6] for explicit forms). Here we present a modified description of the $x_{\alpha\beta\gamma}$ coefficients. In the modified description, the coefficients $\{x_{000}, x_{100}, x_{010}, x_{001}, x_{110}, x_{101}, x_{011}, x_{111}\}$ require rule components r_1, r_2, r_3, …, r_{27} only, while the other $x_{\alpha\beta\gamma}$ coefficients can be described by partly using the coefficients $\{x_{000}, x_{100}, x_{010}, x_{001}, x_{110}, x_{101}, x_{011}, x_{111}\}$ in addition to the rule components r_1, r_2, r_3, …, r_{27}. The modified description of $x_{\alpha\beta\gamma}$ is as follows:

$$
\begin{aligned}
&x_{000}=r_{14},\ x_{100}=(-r_5+r_{23})/2,\ x_{010}=(-r_{11}+r_{17})/2,\\
&x_{001}=(-r_{13}+r_{15})/2,\ x_{110}=(r_2-r_8-r_{20}+r_{26})/4
\end{aligned}
$$

$$
\begin{aligned}
&x_{101}=(r_4-r_6-r_{22}+r_{24})/4,\ x_{011}=(r_{10}-r_{12}-r_{16}+r_{18})/4,\\
&x_{200}=(r_5+r_{23})/2-x_{000},\ x_{020}=(r_{11}+r_{17})/2-x_{000},\\
&x_{002}=(r_{13}+r_{15})/2-x_{000},\ x_{210}=(-r_2+r_8-r_{20}+r_{26})/4-x_{010},\\
&x_{201}=(-r_4+r_6-r_{22}+r_{24})/4-x_{001},\\
&x_{120}=(-r_2-r_8+r_{20}+r_{26})/4-x_{100},\ x_{021}=(-r_{10}+r_{12}-r_{16}+r_{18})/4-x_{001},\\
&x_{102}=(-r_4-r_6+r_{22}+r_{24})/4-x_{100},\\
&x_{012}=(-r_{10}-r_{12}+r_{16}+r_{18})/4-x_{010},\ x_{111}=(-r_1+r_3+r_7-r_9+r_{19}-r_{21}-r_{25}+r_{27})/8,\\
&x_{220}=(r_2+r_8+r_{20}+r_{26})/4-x_{200}-x_{020}-x_{000},\ x_{202}=(r_4+r_6+r_{22}+r_{24})/4-x_{200}-x_{002}-x_{000},\\
&x_{022}=(r_{10}+r_{12}+r_{16}+r_{18})/4-x_{200}-x_{020}-x_{000},\\
&x_{211}=(r_1-r_3-r_7+r_9+r_{19}-r_{21}-r_{25}+r_{27})/8-x_{011},\\
&x_{121}=(r_1-r_3+r_7-r_9-r_{19}+r_{21}-r_{25}+r_{27})/8-x_{101},\\
&x_{112}=(r_1+r_3-r_7-r_9-r_{19}-r_{21}+r_{25}+r_{27})/8-x_{110},\\
&x_{221}=(-r_1+r_3-r_7+r_9-r_{19}+r_{21}-r_{25}+r_{27})/8\\
&\qquad+(r_4-r_6+r_{10}-r_{12}+r_{16}-r_{18}+r_{22}-r_{24})/4+x_{001},\\
&x_{212}=(-r_1-r_3+r_7+r_9-r_{19}-r_{21}+r_{25}+r_{27})/8\\
&\qquad+(r_2-r_8+r_{10}+r_{12}-r_{16}-r_{18}+r_{20}-r_{26})/4+x_{010},\\
&x_{122}=(-r_1-r_3-r_7-r_9+r_{19}+r_{21}+r_{25}+r_{27})/8\\
&\qquad+(r_2+r_4+r_6+r_8-r_{20}-r_{22}-r_{24}-r_{26})/4+x_{100},\\
&x_{222}=(r_1+r_3+r_7+r_9+r_{19}+r_{21}+r_{25}+r_{27})/8-x_{220}-x_{202}-x_{022}-x_{200}-x_{020}-x_{002}-x_{000}.
\end{aligned}
\tag{9}
$$

As can be seen from the rewritten relationships (9), the coefficients x_{210}, x_{201}, and x_{120} can be rewritten in terms of the coefficients $\{x_{000}, x_{100}, x_{010}, x_{001}, x_{110}, x_{101}, x_{011}, x_{111}\}$ only. We see the relation between subscripts for right and left side terms, namely, 210 to 120 (110+010) for x_{210}, 201 to 102 (101+001) for x_{201}, and 120 to 012 (011+001) for x_{120}. Then x_{210} and x_{120} are permuted, and that x_{201} has mirror symmetry. We can also see the relationship between rule components and x coefficients for $CA_3{}^2$ of $\{-1, 1\}$. The triplet product terms of eq. (6) plainly disappear when one of input triplets takes the value 0. As long as the input triplet takes one of state levels -1 or 1, the higher-order terms contribute to the determination of the output level.

To see the $\{-1, 1\}$ binary feature explicitly, we can rewrite the expression of rule for $CA_3{}^3$ in the following form:

$$
\begin{aligned}
f(S_{i-1}(t), S_i(t), S_{i+1}(t)) &= f'_{0\pm1}(S_{i-1}(t), S_i(t), S_{i+1}(t))\\
&\quad + S_{i-1}^2(t)S_i^2(t)S_{i+1}^2(t)f_{\pm1}(S_{i-1}(t), S_i(t), S_{i+1}(t)),
\end{aligned}
\tag{10}
$$

where $f'_{0\pm1}(S_{i-1}(t), S_i(t), S_{i+1}(t))$ and $f_{\pm1}(S_{i-1}(t), S_i(t), S_{i+1}(t))$ are defined as:

$$
\begin{aligned}
f'_{0\pm1}(S_{i-1}(t), S_i(t), S_{i+1}(t)) &= r_{14}(1-S_{i-1}^2(t))(1-S_i^2(t))(1-S_{i+1}^2(t))\\
&\quad +((-r_5+r_{23})/2)S_{i-1}(t)(1-S_i^2(t))(1-S_{i+1}^2(t))\\
&\quad +((-r_{11}+r_{17})/2)(1-S_{i-1}^2(t))S_i(t)(1-S_{i+1}^2(t))\\
&\quad +((-r_{13}+r_{15})/2)(1-S_{i-1}^2(t))(1-S_i^2(t))S_{i+1}(t)
\end{aligned}
$$

$$
\begin{aligned}
&+((r_5+r_{23})/2)S_{i-1}^2(t)(1-S_i^2(t))(1-S_{i+1}^2(t))+((r_{11}+r_{17})/2)(1-S_{i-1}^2(t))S_i^2(t)(1-S_{i+1}^2(t))\\
&+((r_{13}+r_{15})/2)(1-S_{i-1}^2(t))(1-S_i^2(t))S_{i+1}^2(t)+((r_2-r_8-r_{20}+r_{26})/4)S_{i-1}(t)S_i(t)(1-S_{i+1}^2(t))\\
&+((r_4-r_6-r_{22}+r_{24})/4)S_{i-1}(t)(1-S_i^2(t))S_{i+1}(t)\\
&\qquad+((r_{10}-r_{12}-r_{16}+r_{18})/4)(1-S_{i-1}^2(t))S_i(t)S_{i+1}(t)\\
&+((-r_2+r_8-r_{20}+r_{26})/4)S_{i-1}^2(t)S_i(t)(1-S_{i+1}^2(t))\\
&\qquad+((-r_4+r_6-r_{22}+r_{24})/4)S_{i-1}^2(t)(1-S_i^2(t))S_{i+1}(t)\\
&+((-r_2-r_8+r_{20}+r_{26})/4)S_{i-1}(t)S_i^2(t)(1-S_{i+1}^2(t))\\
&\qquad+((-r_{10}+r_{12}-r_{16}+r_{18})/4)(1-S_{i-1}^2(t))S_i^2(t)S_{i+1}(t)\\
&+((-r_4-r_6+r_{22}+r_{24})/4)S_{i-1}(t)(1-S_i^2(t))S_{i+1}^2(t)\\
&\qquad+((-r_{10}-r_{12}+r_{16}+r_{18})/4)(1-S_{i-1}^2(t))S_i(t)S_{i+1}^2(t)\\
&+((r_2+r_8+r_{20}+r_{26})/4)S_{i-1}^2(t)S_i^2(t)(1-S_{i+1}^2(t))\\
&\qquad+((r_4+r_6+r_{22}+r_{24})/4)S_{i-1}^2(t)(1-S_i^2(t))S_{i+1}^2(t)\\
&+((r_{10}+r_{12}+r_{16}+r_{18})/4)(1-S_{i-1}^2(t))S_i^2(t)S_{i+1}^2(t),
\end{aligned}
\tag{11}
$$

$$
\begin{aligned}
f_{\pm1}(S_{i-1}(t),\,S_i(t),\,S_{i+1}(t))=&(1/8)(-r_1+r_3+r_7-r_9+r_{19}-r_{21}-r_{25}+r_{27})S_{i-1}(t)S_i(t)S_{i+1}(t)\\
&+(1/8)(r_1-r_3-r_7+r_9+r_{19}-r_{21}-r_{25}+r_{27})S_i(t)S_{i+1}(t)\\
&+(1/8)(r_1-r_3+r_7-r_9-r_{19}+r_{21}-r_{25}+r_{27})S_{i-1}(t)S_{i+1}(t)\\
&+(1/8)(r_1+r_3-r_7-r_9-r_{19}-r_{21}+r_{25}+r_{27})S_{i-1}(t)S_i(t)\\
&+(1/8)(-r_1+r_3-r_7+r_9-r_{19}+r_{21}-r_{25}+r_{27})S_{i+1}(t)\\
&+(1/8)(-r_1-r_3+r_7+r_9-r_{19}-r_{21}+r_{25}+r_{27})S_i(t)\\
&+(1/8)(-r_1-r_3-r_7-r_9+r_{19}+r_{21}+r_{25}+r_{27})S_{i-1}(t)\\
&+(1/8)(r_1+r_3+r_7+r_9+r_{19}+r_{21}+r_{25}+r_{27}).
\end{aligned}
\tag{12}
$$

Note that $f_{\pm1}(S_{i-1}(t), S_i(t), S_{i+1}(t))$ refers to binary $\{-1, 1\}$ CA rules and $f'_{0\pm1}(S_{i-1}(t), S_i(t), S_{i+1}(t))$ denotes the remaining terms of the rule for ternary CA ($CA_3{}^3$) after collecting binary $\{-1, 1\}$ behavior terms. It is known from the expression (10) that the binary term $f_{\pm1}(S_{i-1}(t), S_i(t), S_{i+1}(t))$ always drops out when at least one of term in the input triplet $(S_{i-1}(t), S_i(t), S_{i+1}(t))$ takes the level 0. In other words, the binary term $f_{\pm1}(S_{i-1}(t), S_i(t), S_{i+1}(t))$ survives only when all the members of the input triplet take one of the levels -1 or 1. The property given by collapsing to $CA_3{}^2$ rules occurs by the state level distribution in the cell array.

3. Spatio-Temporal Patterns Appearing in Ternary Cellular Automata

We firstly encountered ternary cellular automata in a study of discrete effects resembling those of the nonlinear Schrödinger equation (NLSE) [3]. The binary blocks $1-1$ and -11 in the "sea" of 0 s move to the right and the left directions respectively, and they pass through each other after collisions [3], like solitons of the continuous NLSE, when the rule satisfies the condition that $r_2=r_{10}$, $r_3=r_{19}$, $r_5=r_{13}=-1$, $r_6=r_{22}$, $r_8=r_{16}=0$, $r_9=r_{25}$, $r_{12}=r_{20}=1$, $r_{15}=r_{23}=0$, $r_{18}=r_{26}$, $r_4=-1$, $r_{11}=1$, $r_{14}=0$, $r_{21}=-1$, $r_{24}=0$. Since we had the general scheme of CA rule description [3,4], we can investigate cellular automata in a systematic way.

As expected from Wolfram's works [5], many rules of $CA_3{}^3$ give apparently similar spatio-temporal patterns. We have been carrying out a numerical study for the patterns of ternary cellular automata as ternary texture stimuli for visual science studies [6]. The entire numerical study of ternary cellular automata has not been completed due to the large number of CA_3^3 rules. Here we show examples of spatio-temporal patterns from the study of ternary textures [6]. The examples presented are a small subset of the ternary textures that we have investigated. In the texture study, a recurrence rule of the input triplet to the output pixel is applied to an initially-random ternary two-dimensional pixel array. Since a texture is a two-dimensional object, two-dimensional (2D) geometry may be considered for the recurrence rule. We call a 2D recurrence rule a "glider". The Wolfram type cellular automata (Wolfram CA) produces spatio-temporal patterns by 2D recurrence rules if one-dimensional space and time (1D space, time) is to be assigned to two-dimensional space (x, y). The Wolfram glider in our texture study is identical to the recurrence equation (eq. (1)). The textures given by the Wolfram glider therefore are the spatio-temporal patterns of a Wolfram CA with random initial configuration of cell states and random boundary conditions.

Figure 2 shows examples of spatio-temporal patterns of ternary Wolfram CA. As seen from the subfigures, the well-known Wolfram CA patterns are seen in a localized way. These spatio-temporal patterns are obtained by the following rule:

$$\begin{aligned}
&f(S_{i-1}(t), S_i(t), S_{i+1}(t)) \\
&\quad = x_{110}S_{i-1}(t)S_i(t) + x_{101}S_{i-1}(t)S_{i+1}(t) + x_{011}S_i(t)S_{i+1}(t) + x_{220}S_{i-1}^2(t)S_i^2(t) \\
&\quad + x_{211}S_{i-1}^2(t)S_i(t)S_{i+1}(t) + x_{121}S_{i-1}(t)S_i^2(t)S_{i+1}(t) + x_{112}S_{i-1}(t)S_i(t)S_{i+1}^2(t) \\
&\quad + x_{202}S_{i-1}^2(t)S_{i+1}^2(t) + x_{022}S_i^2(t)S_{i+1}^2(t) + x_{222}S_{i-1}^2(t)S_i^2(t)S_{i+1}^2(t) \qquad (13) \\
&\quad = x_{110}S_{i-1}(t)S_i(t) + x_{101}S_{i-1}(t)S_{i+1}(t) + x_{011}S_i(t)S_{i+1}(t) \\
&\quad + S_{i-1}^2(t)S_i^2(t)S_{i+1}^2(t)(x_{112}S_{i-1}(t)S_i(t) + x_{121}S_{i-1}(t)S_{i+1}(t) + x_{211}S_i(t)S_{i+1}(t) + x_{222}) \\
&\quad + x_{220}S_{i-1}^2(t)S_i^2(t) + x_{202}S_{i-1}^2(t)S_{i+1}^2(t) + x_{022}S_i^2(t)S_{i+1}^2(t), \qquad (14)
\end{aligned}$$

$$\begin{aligned}
&x_{110} = (r_2 - r_8 - r_{20} + r_{26})/4,\ x_{101} = (r_4 - r_6 - r_{22} + r_{24})/4,\ x_{011} = (r_{10} - r_{12} - r_{16} + r_{18})/4, \\
&x_{211} = (r_1 - r_3 - r_7 + r_9 + r_{19} - r_{21} - r_{25} + r_{27})/8 - x_{011}, \\
&x_{121} = (r_1 - r_3 + r_7 - r_9 - r_{19} + r_{21} - r_{25} + r_{27})/8 - x_{101}, \\
&x_{112} = (r_1 + r_3 - r_7 - r_9 - r_{19} - r_{21} + r_{25} + r_{27})/8 - x_{110}, \\
&x_{220} = (r_2 + r_8 + r_{20} + r_{26})/4 - x_{200} - x_{020} - x_{000}, \\
&x_{202} = (r_4 + r_6 + r_{22} + r_{24})/4 - x_{200} - x_{002} - x_{000}, \\
&x_{022} = (r_{10} + r_{12} + r_{16} + r_{18})/4 - x_{200} - x_{020} - x_{000}, \\
&x_{222} = (r_1 + r_3 + r_7 + r_9 + r_{19} + r_{21} + r_{25} + r_{27})/8 - x_{220} - x_{202} - x_{022} - x_{200} - x_{020} - x_{002} - x_{000}, \\
&x_{000} = r_{14},\ x_{200} = (r_5 + r_{23})/2 - x_{000},\ x_{020} = (r_{11} + r_{17})/2 - x_{000},\ x_{002} = (r_{13} + r_{15})/2 - x_{000}. \qquad (15)
\end{aligned}$$

The spatio-temporal patterns are *banded* binary Wolfram CA, that is the spatio-temporal patterns of CA_3^2 by $\{-1, 1\}$ are separated by gray stripes. These patterns are a developed version of class 2 in CA_3^3 from class 2 of CA_3^2 [1]. These patterns cannot be generated within CA_3^2 of the Wolfram type.

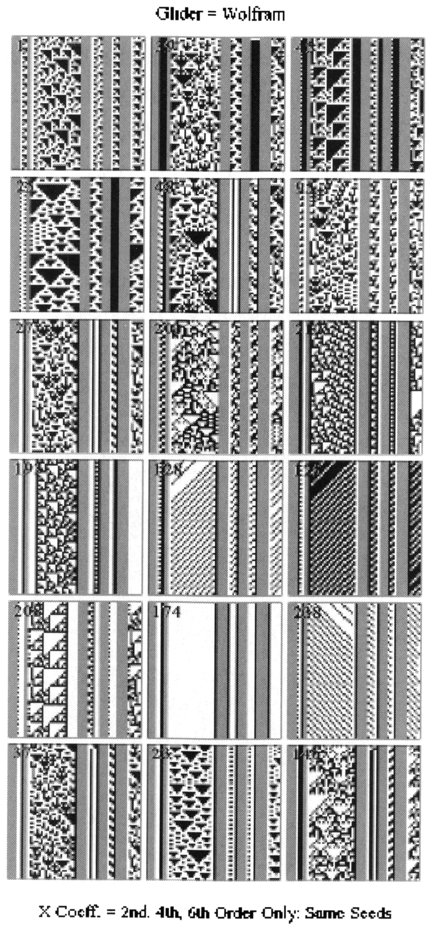

Figure 2 Patterns of Locally Binary CA in CA_3^3

From eq. (14), if $x_{110}=x_{112}$, $x_{101}=x_{121}$, and $x_{011}=x_{211}$ then $f(S_{i-1}(t), S_i(t), S_{i+1}(t))$ includes the term $(x_{110}S_{i-1}(t)S_i(t)+x_{101}S_{i-1}(t)S_{i+1}(t)+x_{011}S_i(t)S_{i+1}(t))(1+S_{i-1}^2(t)S_i^2(t)S_{i+1}^2(t))$. This fact implies that the decomposed factor $x_{110}S_{i-1}(t)S_i(t)+x_{101}S_{i-1}(t)S_{i+1}(t)+x_{011}S_i(t)S_{i+1}(t)$ is always significant, because another factor $(1+S_{i-1}^2(t)S_i^2(t)S_{i+1}^2(t))$ takes the value 1 when at least one of input triplet cells takes the value 0, and that takes the value 2 when all the input triplet cells take the value -1 or 1. The other terms of eq. (14), $x_{220}S_{i-1}^2(t)S_i^2(t)+x_{202}S_{i-1}^2(t)S_{i+1}^2(t)+x_{022}S_i^2(t)S_{i+1}^2(t)$, behave like a binary {0, 1} CA. Thus we know that localized patterns are generated by the terms $x_{110}S_{i-1}(t)S_i(t)+x_{101}S_{i-1}(t)S_{i+1}(t)+x_{011}S_i(t)S_{i+1}(t)$.

Spatio-temporal patterns of Figure 3 are true ternary patterns. except for the top LinSam1 (4th horizontal row) and LinSam3 (6th horizontal row) clearly show locally ternary patterns. The third picture of LinSam1 shows the behavior of class 4 on chaotic temporal development of cell states (class 3). The pictures on the top row are binary patterns, namely, spatio-temporal patterns of CA_3^2 by $\{-1, 1\}$ with random boundary conditions. These binary patterns are a part of Wolfram CA patterns, but the boundary conditions are different. The Rloc and LinSam are the name for several groups that are explained below.

Rloc26 means that $r_2=r_4=r_5=r_{10}=r_{11}=r_{13}=1$ for $\{-1, 0\}$ triplets, $r_3=r_7=r_9=r_{19}=r_{21}=r_{25}=0$ for $\{-1, 1\}$ triplets, $r_{15}=r_{17}=r_{18}=r_{23}=r_{24}=r_{26}=-1$ for $\{0, 1\}$ triplets, two -1s,

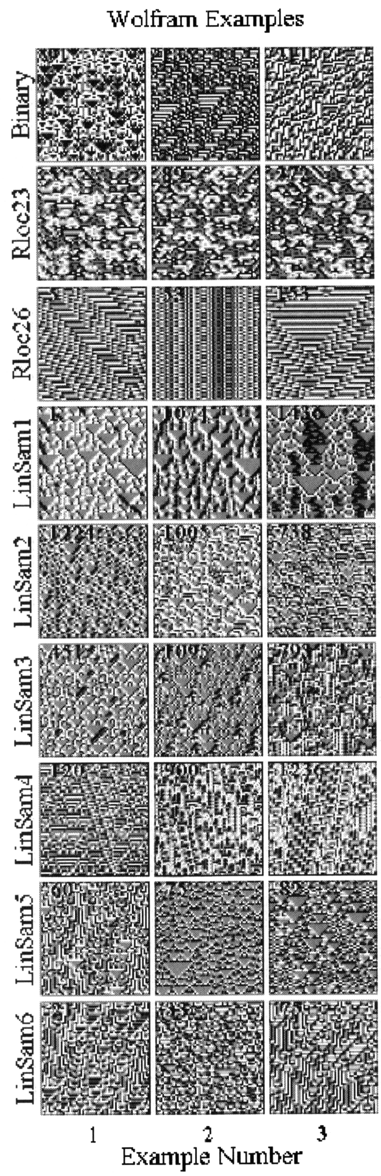

Figure 3 Selected Spatio-Temporal Patterns in CA_3^3

two 0s, and two 1s for $\{r_6, r_8, r_{12}\ r_{16}, r_{20}, r_{22}\}$, and $(r_1, r_{14}, r_{27}) \in \{(-1, 0, 1), (-1, 1, 0), (0, -1, 1), (0, 1, -1), (1, -1, 0), (1, 0, -1)\}$. Rloc23 means that $r_2 = r_4 = r_5 = r_{10} = r_{11} = r_{13} = 0$ for $\{-1, 0\}$ triplets, $r_3 = r_7 = r_9 = r_{19} = r_{21} = r_{25} = -1$ for $\{-1, 1\}$ triplets, $r_{15} = r_{17} = r_{18} = r_{23} = r_{24} = r_{26} = 1$ for $\{0, 1\}$ triplets, two -1s, two 0s, and two 1s for $\{r_6, r_8, r_{12}\ r_{16}, r_{20}, r_{22}\}$, and $(r_1, r_{14}, r_{27}) \in \{(-1, 0, 1), (-1, 1, 0), (0, -1, 1), (0, 1, -1), (1, -1, 0), (1, 0, -1)\}$. The name LinSam means that the x_{100}, x_{010} and x_{001} coefficients of the linear terms are all zero. The rule LinSam satisfies that $r_5 = r_{23}$, $r_{11} = r_{17}$, and $r_{13} = r_{15}$, from the equation (9) which denotes the relationships between x coefficients and rule components r_i $(i = 1, 2, \ldots, 27)$. The rule components that are not specified in Table 2 are used as parameters that take one of the values $\{-1, 0, 1\}$. The rule components r_5 $(= r_{23})$, r_{11} $(= r_{17})$, and r_{13} $(= r_{15})$ also take the value of one of integers -1, 0, and 1. The other rule components for LinSam1–6 are listed in Table 2.

Table 2 List of LinSam 1 to LinSam 6 Conditions

LinSam 1	LinSam 2	LinSam 3	LinSam 4	LinSam 5	LinSam 6
$x_{100} = x_{010} = x_{001} = 0$, $[x_{100} = (-r_5 + r_{23})/2$, $x_{010} = (-r_{11} + r_{17})/2$, $x_{001} = (-r_{13} + r_{15})/2]$					
$r_1 = r_{14} = r_{27} = 0$	$r_1 = 1$, $r_{14} = 0$, $r_{27} = -1$		$r_1 = 1$, $r_{14} = -1$ or 1 $r_{27} = -1$	$r_1 = r_{14} = r_{27} = 0$	$r_{14} = -1$ or 1 $r_1 = r_{27} = 0$
$r_3 = r_7 = r_9 = r_{19} = r_{21} = r_{25} = 0$				$r_3 = r_7 = r_{19} = 1$, $r_9 = r_{21} = r_{25} = -1$	
	$r_2 = r_4 = 0$	$r_2 = r_6 = 0$	$r_2 = r_4 = r_{26} = 0$		$r_6 = 0$

The LinSam1–6 rules generate wide range of patterns in addition to the patterns shown in Fig. 3. Figure 4 shows the patterns obtained for the propagating local structures and their collisions. These patterns are selected from the LinSam 3 pictures. As seen from Fig. 4, there are many types of propagating local structures. For example, some propagating local structures are large, some of them are like sea waves, some of them propagate while emitting beams, some of them show an alternation of appearing and disappearing of local structures in a wavy sea, and some show complicated local structures that propagate in a chaotic manner.

We expect that the fastest propagation of a local structure is 1 site-shift per unit time from the recurrence equation (eq. (1)) for neighborhood three CA. The propagation velocities for larger local structures are slower than 1 site-shift per unit time. The propagation velocity of 1 site-shift per unit time is seen in the dislocations included in wavy lines. However we recognize that the wavy lines are faster propagators than the velocity of 1 site-shift per unit time. The wavy lines are modification of horizontal stripe lines just like the birth-death process. The horizontal lines mean an infinite limit of the structure propagation. The wavy lines therefore move faster than 1 site-shift per unit time. Thus a faster case than 1 site-shift per unit time only occurs for wavy lines. Hence we knew that the wavy lines form quite a large-scale structure with respect to the space direction.

In the Rloc26 rule, every binary triplet input gives an output of excluding integers except for the input triplets $(-1, -1, -1)$, $(0, 0, 0)$, and $(1, 1, 1)$. Thus it is expected that the Rloc26 rule may not cause any large local structures. This rule produces wavy lines or vertical

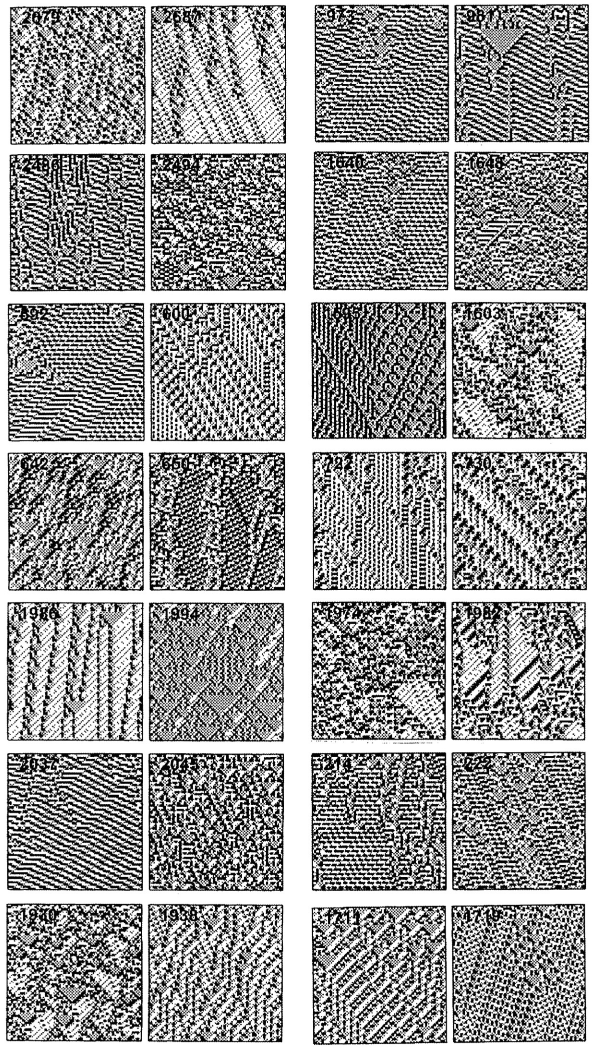

Figure 4 Propagating Local Structures in LinSam Spatio-Temporal Patterns

stripe lines like standing solitons, since the rule requires rapid change of state in each cell. Actually the Rloc26 rule generates many such kind of patterns. But the Rloc26 rule generates chaotic triangular patterns that are seen in Wolfram CA [7]. The chaotic triangle patterns are consisting of white, black, and gray triangles [7]. This should be a feature expected from the exclusion property of the Rloc26 rule.

The patterns of ternary cellular automata are similar to those of binary cellular automata worked by Wolfram [5]: triangles appearing in chaotic spatio- temporal patterns are typical in $CA_3{}^2$. We cannot say what is a typical pattern in $CA_3{}^3$. We have not inspected the all the patterns generated by the rules of $CA_3{}^3$, but probably we have explored the major patterns of CA_3^3. We may explain the patterns in CA_3^3 by the some manipulation of the patterns generated by CA_3^2. This is expected from the written form of the rule, eq. (10). The remaining point is how to predict what type of spatio-temporal pattern a given rule will generate.

4. Conclusion

We have studied a selection of the spatio-temporal patterns for ternary CA with three neighbors on a strategy to investigate, because there are 7.6256×10^{12} the entire discrete functions (i.e., rules). Our strategy in the current study is based on the $x_{\alpha\beta\gamma}$ coefficients appearing in eq. (6). We eliminate the linear terms of eq. (6). The *banded* binary CA patterns appear when we eliminate the 1st, 3rd, 5th order of eq. (6). LinSam was just named for setting the linear terms represented with the summation of rule components (see Table 2) to be zero. The LinSam rules can generate complicated spatio-temporal patterns shown in Figs 3 and 4. We furthermore used a guideline to reduce the computation load, *viz*. an even assignment of rule components to the integers $\{-1, 0, 1\}$. In other words, the 27 rule components in CA_3^3 were assigned so that 9 of them are -1, 9 of the remaining 18 components are 0, and finally the remaining 9 components are 1. Then, for example, the number of generated patterns was 5192 in LinSam1 rules [6]. Consequently, we were able to avoid having many trivial spatio-temporal patterns in CA_3^3. There exist 7.6256×10^{12} rules as mentioned, so we have investigated a few of them. From the well-known Wolfram work [5], we knew that many rules generate the same pattern or quite similar patterns, apart from a short initial transient. Our strategy used here avoids this repetition. However we need to know what kind of rules generate the same pattern or almost the same pattern in order to understand the feature of ternary cellular automata. This remains a task for our future investigations.

References

[1] Wolfram, S., "Universality and complexity in cellular automata", *Physica* **10D**, 1–35, (1984).
[2] Badii, R., Politi, A., *Complexity* section 3.4, Cambridge U press, UK, 1997.
[3] Ankiewicz, A., Nagai, Y., "Solitons in multi-level cellular automata", *Chaos Solitons and Fractals* **13**, 1345–1358, (2002).
[4] Nagai, Y., Maddess, T., Ankiewicz, A., "Discrete algebra on cellular automata and binary textures", *Mem Kokushikan U Cent Inform Sci*, **22**, 51–64, (2001).
[5] Wolfram, S., *Theory and Applications of Cellular automata*, World scientific, Singapore, 1986.
[6] Maddess, T., Nagai, Y., Ankiewicz, A., James, A. C., "Binary and ternary textures containing higher order spatial correlations", submitted to *Vision Research*.
[7] Nagai, Y., Ankiewicz, A., Maddess, T., "A complete rule description for Ternary Cellular Automata and selected spatio-temporal patterns", in preparation.